EfficientFormer: Vision Transformers at MobileNet Speed

Yanyu Li[1,2,†] **Geng Yuan**[1,2,†] **Yang Wen**[1] **Ju Hu**[1] **Georgios Evangelidis**[1]
Sergey Tulyakov[1] **Yanzhi Wang**[2] **Jian Ren**[1]
[1]Snap Inc. [2]Northeastern University

Abstract

Vision Transformers (ViT) have shown rapid progress in computer vision tasks, achieving promising results on various benchmarks. However, due to the massive number of parameters and model design, *e.g.*, attention mechanism, ViT-based models are generally times slower than lightweight convolutional networks. Therefore, the deployment of ViT for real-time applications is particularly challenging, especially on resource-constrained hardware such as mobile devices. Recent efforts try to reduce the computation complexity of ViT through network architecture search or hybrid design with MobileNet block, yet the inference speed is still unsatisfactory. This leads to an important question: *can transformers run as fast as MobileNet while obtaining high performance?* To answer this, we first revisit the network architecture and operators used in ViT-based models and identify inefficient designs. Then we introduce a dimension-consistent pure transformer (without MobileNet blocks) as a design paradigm. Finally, we perform latency-driven slimming to get a series of final models dubbed EfficientFormer. Extensive experiments show the superiority of EfficientFormer in performance and speed on mobile devices. Our fastest model, EfficientFormer-L1, achieves 79.2% top-1 accuracy on ImageNet-1K with only 1.6 ms inference latency on iPhone 12 (compiled with CoreML), which runs as fast as MobileNetV2×1.4 (1.6 ms, 74.7% top-1), and our largest model, EfficientFormer-L7, obtains 83.3% accuracy with only 7.0 ms latency. Our work proves that properly designed transformers can reach *extremely low latency* on mobile devices while maintaining *high performance*[1].

1 Introduction

The transformer architecture [1], initially designed for Natural Language Processing (NLP) tasks, introduces the Multi-Head Self Attention (MHSA) mechanism that allows the network to model long-term dependencies and is easy to parallelize. In this context, Dosovitskiy *et al.* [2] adapt the attention mechanism to 2D images and propose Vision Transformer (ViT): the input image is divided into non-overlapping patches, and the inter-patch representations are learned through MHSA without inductive bias. ViTs demonstrate promising results compared to convolutional neural networks (CNNs) on computer vision tasks. Following this success, several efforts explore the potential of ViT by improving training strategies [3, 4, 5], introducing architecture changes [6, 7], redesigning attention mechanisms [8, 9], and elevating the performance of various vision tasks such as classification [10, 11, 12], segmentation [13, 14], and detection [15, 16].

On the downside, transformer models are usually times slower than competitive CNNs [17, 18]. There are many factors that limit the inference speed of ViT, including the massive number of

[†]These authors contributed equally.
[1]Code and models are available at https://github.com/snap-research/EfficientFormer.

36th Conference on Neural Information Processing Systems (NeurIPS 2022).

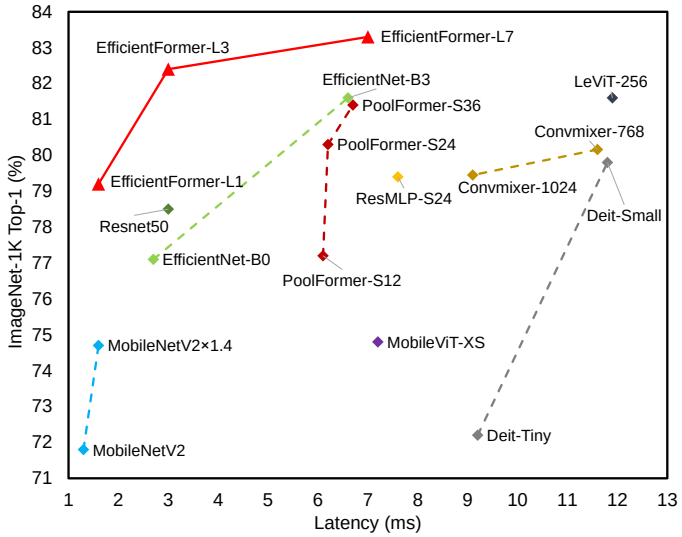

Figure 1: **Inference Speed *vs.* Accuracy.** All models are trained on ImageNet-1K and measured by iPhone 12 with CoreMLTools to get latency. Compared to CNNs, EfficientFormer-L1 runs 40% faster than EfficientNet-B0, while achieves 2.1% higher accuracy. For the latest MobileViT-XS, EfficientFormer-L7 runs 0.2 ms faster with 8.5% higher accuracy.

parameters, quadratic-increasing computation complexity with respect to token length, non-foldable normalization layers, and lack of compiler level optimizations (*e.g.*, Winograd for CNN [19]). The high latency makes transformers impractical for real-world applications on resource-constrained hardware, such as augmented or virtual reality applications on mobile devices and wearables. As a result, lightweight CNNs [20, 21, 22] remain the default choice for real-time inference.

To alleviate the latency bottleneck of transformers, many approaches have been proposed. For instance, some efforts consider designing new architectures or operations by changing the linear layers with convolutional layers (CONV) [23], combining self-attention with MobileNet blocks [24], or introducing sparse attention [25, 26, 27], to reduce the computational cost, while other efforts leverage network searching algorithm [28] or pruning [29] to improve efficiency. Although the computation-performance trade-off has been improved by existing works, the fundamental question that relates to the applicability of transformer models remains unanswered: *Can powerful vision transformers run at MobileNet speed and become a default option for edge applications?* This work provides a study towards the answer through the following contributions:

- First, we revisit the design principles of ViT and its variants through latency analysis (Sec. 3). Following existing work [18], we utilize iPhone 12 as the testbed and publicly available CoreML [30] as the compiler, since the mobile device is widely used and the results can be easily reproduced.
- Second, based on our analysis, we identify inefficient designs and operators in ViT and propose a new dimension-consistent design paradigm for vision transformers (Sec. 4.1).
- Third, starting from a supernet with the new design paradigm, we propose a simple yet effective latency-driven slimming method to obtain a new family of models, namely, EfficientFormers (Sec. 4.2). We directly optimize for inference speed instead of MACs or number of parameters [31, 32, 33].

Our fastest model, EfficientFormer-L1, achieves 79.2% top-1 accuracy on ImageNet-1K [34] classification task with only 1.6 ms inference time (averaged over $1,000$ runs), which runs as fast as MobileNetV2×1.4 and wields 4.5% *higher* top-1 accuracy (more results in Fig. 1 and Tab. 1). The promising results demonstrate that latency is no longer an obstacle for the widespread adoption of vision transformers. Our largest model, EfficientFormer-L7, achieves 83.3% accuracy with only 7.0 ms latency, outperforms ViT×MobileNet hybrid designs (MobileViT-XS, 74.8%, 7.2ms) by a large margin. Additionally, we observe superior performance by employing EfficientFormer as

the backbone in image detection and segmentation benchmarks (Tab. 2). We provide a preliminary answer to the aforementioned question, *ViTs can achieve ultra fast inference speed and wield powerful performance at the same time.* We hope our EfficientFormer can serve as a strong baseline and inspire followup works on the edge deployment of vision transformers.

2 Related Work

Transformers are initially proposed to handle the learning of long sequences in NLP tasks [1]. Dosovitskiy *et al.* [2] and Carion *et al.* [15] adapt the transformer architecture to classification and detection, respectively, and achieve competitive performance against CNN counterparts with stronger training techniques and larger-scale datasets. DeiT [3] further improves the training pipeline with the aid of distillation, eliminating the need for large-scale pretraining [35]. Inspired by the competitive performance and global receptive field of transformer models, follow-up works are proposed to refine the architecture [36, 37], explore the relationship between CONV nets and ViT [38, 39, 40], and adapt ViT to different computer vision tasks [13, 41, 42, 43, 44, 45, 46]. Other research efforts explore the essence of attention mechanism and propose insightful variants of token mixer, *e.g.*, local attention [8], spatial MLP [47, 48], and pooling-mixer [6].

Despite the success in most vision tasks, ViT-based models cannot compete with the well-studied lightweight CNNs [21, 49] when the inference speed is the major concern [50, 51, 52], especially on resource-constrained edge devices [17]. To accelerate ViT, many approaches have been introduced with different methodologies, such as proposing new architectures or modules [53, 54, 55, 56, 57, 58], re-thinking self-attention and sparse-attention mechanisms [59, 60, 61, 62, 63, 64, 65], and utilizing search algorithms that are widely explored in CNNs to find smaller and faster ViTs [66, 28, 29, 67]. Recently, LeViT [23] proposes a CONV-clothing design to accelerate vision transformer. However, in order to perform MHSA, the 4D features need to be frequently reshaped into flat patches, which is still expensive to compute on edge resources (Fig. 2). Likewise, MobileViT [18] introduces a hybrid architecture that combines lightweight MobileNet blocks (with point-wise and depth-wise CONV) and MHSA blocks; the former is placed at early stages in the network pipeline to extract low-level features, while the latter is placed in late stages to enjoy the global receptive field. Similar approach has been explored by several works [24, 28] as a straightforward strategy to reduce computation.

Different from existing works, we aim at pushing the latency-performance boundary of pure vision transformers instead of relying on hybrid designs, and directly optimize for mobile latency. Through our detailed analysis (Sec. 3), we propose a new design paradigm (Sec. 4.1), which can be further elevated through architecture search (Sec. 4.2).

3 On-Device Latency Analysis of Vision Transformers

Most existing approaches optimize the inference speed of transformers through computation complexity (MACs) or throughput (images/sec) obtained from server GPU [23, 28]. While such metrics do not reflect the real on-device latency. To have a clear understanding of which operations and design choices slow down the inference of ViTs on edge devices, we perform a comprehensive latency analysis over a number of models and operations, as shown in Fig. 2, whereby the following observations are drawn.

Observation 1: *Patch embedding with large kernel and stride is a speed bottleneck on mobile devices.*

Patch embedding is often implemented with a non-overlapping convolution layer that has large kernel size and stride [3, 55]. A common belief is that the computation cost of the patch embedding layer in a transformer network is unremarkable or negligible [2, 6]. However, our comparison in Fig. 2 between models with large kernel and stride for patch embedding, *i.e.*, DeiT-S [3] and PoolFormer-S24 [6], and the models without it, *i.e.*, LeViT-256 [23] and EfficientFormer, shows that patch embedding is instead a speed bottleneck on mobile devices.

Large-kernel convolutions are not well supported by most compilers and cannot be accelerated through existing algorithms like Winograd [19]. Alternatively, the non-overlapping patch embedding can be replaced by a convolution stem with fast downsampling [68, 69, 23] that consists of several hardware-efficient 3×3 convolutions (Fig. 3).

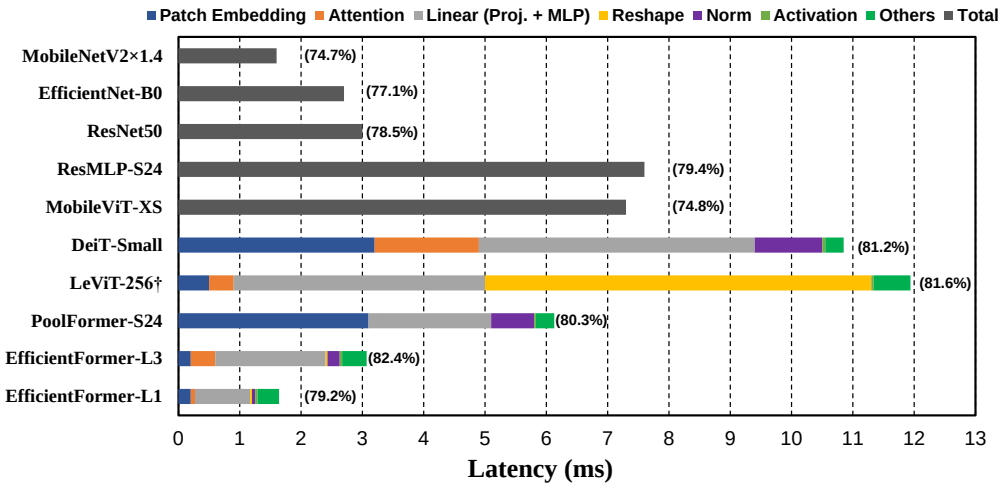

Figure 2: **Latency profiling.** Results are obtained on iPhone 12 with CoreML. The on-device speed for CNN (MobileNetV2×1.4, ResNet50, and EfficientNet-B0), ViT-based models (DeiT-Small, LeViT-256, PoolFormer-S24, and EfficientFormer), and various operators are reported. The latency of models and operations are denoted with different color. $(\cdot)$ is the top-1 accuracy on ImageNet-1K. †LeViT uses HardSwish which is not well supported by CoreML, we replace it with GeLU for fair comparison.

Observation 2: *Consistent feature dimension is important for the choice of token mixer. MHSA is not necessarily a speed bottleneck.*

Recent work extends ViT-based models to the MetaFormer architecture [6] consisting of MLP blocks and unspecified token mixers. Selecting a token mixer is an essential design choice when building ViT-based models. The options are many—the conventional MHSA mixer with a global receptive field, more sophisticated shifted window attention [8], or a non-parametric operator like pooling [6].

We narrow the comparison to the two token mixers, pooling and MHSA, where we choose the former for its simplicity and efficiency, while the latter for better performance. More complicated token mixers like shifted window [8] are currently not supported by most public mobile compilers and we leave them outside our scope. Furthermore, we do not use depth-wise convolution to replace pooling [70] as we focus on building architecture without the aid of lightweight convolutions.

To understand the latency of the two token mixers, we perform the following two comparisons:

- First, by comparing PoolFormer-s24 [6] and LeViT-256 [23], we observe that the `Reshape` operation is a bottleneck for LeViT-256. The majority of LeViT-256 is implemented with CONV on 4D tensor, requiring frequent reshaping operations when forwarding features into MHSA since the attention has to be performed on patchified 3D tensor (discarding the extra dimension of attention heads). The extensive usage of `Reshape` limits the speed of LeViT on mobile devices (Fig. 2). On the other hand, pooling naturally suits the 4D tensor when the network primarily consists of CONV-based implementations, *e.g.*, CONV 1×1 as MLP implementation and CONV stem for downsampling. As a result, PoolFormer exhibits faster inference speed.
- Second, by comparing DeiT-Small [3] and LeViT-256 [23], we find that MHSA does not bring significant overhead on mobiles if the feature dimensions are consistent and `Reshape` is not required. Though much more computation intensive, DeiT-Small with a consistent 3D feature can achieve comparable speed to the new ViT variant, *i.e.*, LeViT-256.

In this work, we propose a dimension-consistent network (Sec. 4.1) with both 4D feature implementation and 3D MHSA, but the inefficient frequent `Reshape` operations are eliminated.

Observation 3: *CONV-BN is more latency-favorable than LN (GN)-Linear and the accuracy drawback is generally acceptable.*

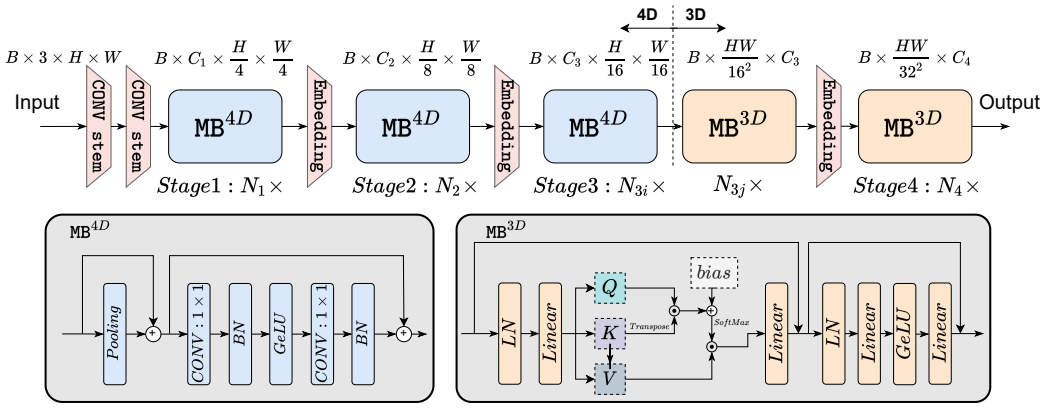

Figure 3: **Overview of EfficientFormer.** The network starts with a convolution stem as patch embedding, followed by MetaBlock (MB). The $\texttt{MB}^{4D}$ and $\texttt{MB}^{3D}$ contain different token mixer configurations, *i.e.*, local pooling or global multi-head self-attention, arranged in a dimension-consistent manner.

Choosing the MLP implementation is another essential design choice. Usually, one of the two options is selected: layer normalization (LN) with 3D linear projection (proj.) and CONV 1×1 with batch normalization (BN). CONV-BN is more latency favorable because BN can be folded into the preceding convolution for inference speedup, while dynamic normalizations, such as LN and GN, still collects running statistics at the inference phase, thus contributing to latency. From the analysis of DeiT-Small and PoolFormer-S24 in Fig. 2 and previous work [17], the latency introduced by LN constitutes around $10\% - 20\%$ latency of the whole network.

Based on our ablation study in Appendix Tab. 3, CONV-BN only slightly downgrades performance compared to GN and achieves comparable results to channel-wise LN. In this work, we apply CONV-BN as much as possible (in all latent 4D features) for the latency gain with a negligible performance drop, while using LN for the 3D features, which aligns with the original MHSA design in ViT and yields better accuracy.

Observation 4: *The latency of nonlinearity is hardware and compiler dependent.*

Lastly, we study nonlinearity, including GeLU, ReLU, and HardSwish. Previous work [17] suggests GeLU is not efficient on hardware and slows down inference. However, we observe GeLU is well supported by iPhone 12 and hardly slower than its counterpart, ReLU. On the contrary, HardSwish is surprisingly slow in our experiments and may not be well supported by the compiler (LeViT-256 latency with HardSwish is 44.5 ms while with GeLU 11.9 ms). We conclude that nonlinearity should be determined on a case-by-case basis given specific hardware and compiler at hand. We believe that most of the activations will be supported in the future. In this work, we employ GeLU activations.

4 Design of EfficientFormer

Based on the latency analysis, we propose the design of EfficientFormer, demonstrated in Fig. 3. The network consists of a patch embedding (`PatchEmbed`) and stack of meta transformer blocks, denoted as `MB`:

$$\mathcal{Y} = \prod_{i}^{m} \texttt{MB}_i(\texttt{PatchEmbed}(\mathcal{X}_0^{B,3,H,W})), \tag{1}$$

where $\mathcal{X}_0$ is the input image with batch size as B and spatial size as $[H, W]$, $\mathcal{Y}$ is the desired output, and m is the total number of blocks (depth). `MB` consists of unspecified token mixer (`TokenMixer`) followed by a `MLP` block and can be expressed as follows:

$$\mathcal{X}_{i+1} = \texttt{MB}_i(\mathcal{X}_i) = \texttt{MLP}(\texttt{TokenMixer}(\mathcal{X}_i)), \tag{2}$$

where $\mathcal{X}_{i|i>0}$ is the intermediate feature that forwarded into the i^{th} `MB`. We further define Stage (or `S`) as the stack of several MetaBlocks that processes the features with the same spatial size, such as $N_1\times$ in Fig. 3 denoting $\texttt{S}_1$ has N_1 MetaBlocks. The network includes 4 Stages. Among each Stage, there

is an embedding operation to project embedding dimension and downsample token length, denoted as Embedding in Fig. 3. With the above architecture, EfficientFormer is a fully transformer-based model without integrating MobileNet structures. Next, we dive into the details of the network design, specifically, the architecture details and the search algorithm.

4.1 Dimension-Consistent Design

With the observations in Sec. 3, we propose a dimension consistent design which splits the network into a 4D partition where operators are implemented in CONV-net style ($\texttt{MB}^{4D}$), and a 3D partition where linear projections and attentions are performed over 3D tensor to enjoy the global modeling power of MHSA without sacrificing efficiency ($\texttt{MB}^{3D}$), as shown in Fig. 3. Specifically, the network starts with 4D partition, while 3D partition is applied in the last stages. Note that Fig. 3 is just an instance, the actual length of 4D and 3D partition is specified later through architecture search.

First, input images are processed by a CONV stem with two 3×3 convolutions with stride 2 as patch embedding,

$$\mathcal{X}_1^{B,C_{j|j=1},\frac{H}{4},\frac{W}{4}} = \texttt{PatchEmbed}(\mathcal{X}_0^{B,3,H,W}), \tag{3}$$

where C_j is the channel number (width) of the $j\,th$ stage. Then the network starts with $\texttt{MB}^{4D}$ with a simple Pool mixer to extract low level features,

$$\begin{aligned} \mathcal{I}_i &= \texttt{Pool}(\mathcal{X}_i^{B,C_j,\frac{H}{2^{j+1}},\frac{W}{2^{j+1}}}) + \mathcal{X}_i^{B,C_j,\frac{H}{2^{j+1}},\frac{W}{2^{j+1}}}, \\ \mathcal{X}_{i+1}^{B,C_j,\frac{H}{2^{j+1}},\frac{W}{2^{j+1}}} &= \texttt{Conv}_B(\texttt{Conv}_{B,G}(\mathcal{I}_i)) + \mathcal{I}_i, \end{aligned} \tag{4}$$

where $\texttt{Conv}_{B,G}$ refers to whether the convolution is followed by BN and GeLU, respectively. Note here we do not employ Group or Layer Normalization (LN) before the Pool mixer as in [6], since the 4D partition is CONV-BN based design, thus there exists a BN in front of each Pool mixer.

After processing all the $\texttt{MB}^{4D}$ blocks, we perform a one-time reshaping to transform the features size and enter 3D partition. $\texttt{MB}^{3D}$ follows conventional ViT structure, as in Fig. 3. Formally,

$$\begin{aligned} \mathcal{I}_i &= \texttt{Linear}(\texttt{MHSA}(\texttt{Linear}(\texttt{LN}(\mathcal{X}_i^{B,\frac{HW}{4^{j+1}},C_j})))) + \mathcal{X}_i^{B,\frac{HW}{4^{j+1}},C_j}, \\ \mathcal{X}_{i+1}^{B,\frac{HW}{4^{j+1}},C_j} &= \texttt{Linear}(\texttt{Linear}_G(\texttt{LN}(\mathcal{I}_i))) + \mathcal{I}_i, \end{aligned} \tag{5}$$

where $\texttt{Linear}_G$ denotes the Linear followed by GeLU, and

$$\texttt{MHSA}(Q,K,V) = \texttt{Softmax}(\frac{Q \cdot K^T}{\sqrt{C_j}} + b) \cdot V, \tag{6}$$

where Q, K, V represents query, key, and values learned by the linear projection, and b is parameterized attention bias as position encodings.

4.2 Latency Driven Slimming

Design of Supernet. Based on the dimension-consistent design, we build a supernet for searching efficient models of the network architecture shown in Fig. 3 (Fig. 3 shows an example of searched final network). In order to represent such a supernet, we define the MetaPath (MP), which is the collection of possible blocks:

$$\begin{aligned} &\texttt{MP}_{i,j=1,2} \in \{\texttt{MB}_i^{4D}, I_i\}, \\ &\texttt{MP}_{i,j=3,4} \in \{\texttt{MB}_i^{4D}, \texttt{MB}_i^{3D}, I_i\}, \end{aligned} \tag{7}$$

where I represents identity path, j denotes the j^{th} Stage, and i denotes the i^{th} block. The supernet can be illustrated by replacing MB in Fig. 3 with MP.

As in Eqn. 7, in $\texttt{S}_1$ and $\texttt{S}_2$ of the supernet, each block can select from $\texttt{MB}^{4D}$ or I, while in $\texttt{S}_3$ and $\texttt{S}_4$, the block can be $\texttt{MB}^{3D}$, $\texttt{MB}^{4D}$, or I. We only enable $\texttt{MB}^{3D}$ in the last two Stages for two reasons. First, since the computation of MHSA grows quadratically with respect to token length, integrating it in early Stages would largely increase the computation cost. Second, applying the global MHSA to the last Stages aligns with the intuition that early stages in the networks capture low-level features, while late layers learn long-term dependencies.

Searching Space. Our searching space includes C_j (the width of each Stage), N_j (the number of blocks in each Stage, *i.e.*, depth), and last $\mathbb{N}$ blocks to apply $\texttt{MB}^{3D}$.

Searching Algorithm. Previous hardware-aware network searching methods generally rely on hardware deployment of each candidate in search space to obtain the latency, which is time consuming [71]. In this work, we propose a simple, fast yet effective gradient-based search algorithm to obtain a candidate network that just needs to train the supernet for once. The algorithm has three major steps.

First, we train the supernet with Gumbel Softmax sampling [72] to get the importance score for the blocks within each MP, which can be expressed as

$$\mathcal{X}_{i+1} = \sum_n \frac{e^{(\alpha_i^n + \epsilon_i^n)/\tau}}{\sum_n e^{(\alpha_i^n + \epsilon_i^n)/\tau}} \cdot \texttt{MP}_{i,j}(\mathcal{X}_i), \tag{8}$$

where α evaluates the importance of each block in MP as it represents the probability to select a block, *e.g.*, $\texttt{MB}^{4D}$ or $\texttt{MB}^{3D}$ for the i^{th} block. $\epsilon \sim U(0,1)$ ensures exploration, τ is the temperature, and n represents the type of blocks in MP, *i.e.*, $n \in \{4D, I\}$ for $\texttt{S}_1$ and $\texttt{S}_2$, and $n \in \{4D, 3D, I\}$ for $\texttt{S}_3$ and $\texttt{S}_4$. By using Eqn. 8, the derivatives with respect to network weights and α can be computed easily. The training follows the standard recipe (see Sec. 5.1) to obtain the trained weights and architecture parameter α.

Second, we build a latency lookup table by collecting the on-device latency of $\texttt{MB}^{4D}$ and $\texttt{MB}^{3D}$ with different widths (multiples of 16).

Finally, we perform network slimming on the supernet obtained from the first step through latency evaluation using the lookup table. Note that a typical gradient-based searching algorithm simply select the block with largest α [72], which does not fit our scope as it cannot search the width C_j. In fact, constructing a multiple-width supernet is memory-consuming and even unrealistic given that each MP has several branches in our design. Instead of directly searching on the complex searching space, we perform a gradual slimming on the single-width supernet as follows.

We first define the importance score for $\texttt{MP}_i$ as $\frac{\alpha_i^{4D}}{\alpha_i^I}$ and $\frac{\alpha_i^{3D}+\alpha_i^{4D}}{\alpha_i^I}$ for $\texttt{S}_{1,2}$ and $\texttt{S}_{3,4}$, respectively. Similarly, the importance score for each Stage can be obtained by summing up the scores for all MP within the Stage. With the importance score, we define the action space that includes three options: 1) select I for the least important MP, 2) remove the first $\texttt{MB}^{3D}$, and 3) reduce the width of the least important Stage (by multiples of 16). Then, we calculate the resulting latency of each action through lookup table, and evaluate the accuracy drop of each action. Lastly, we choose the action based on *per-latency accuracy drop* ($\frac{-\%}{ms}$). This process is performed iteratively until target latency is achieved. We show more details of the algorithm in Appendix.

5 Experiments and Discussion

We implement EfficientFormer through PyTorch 1.11 [73] and Timm library [74], which is the common practice in recent arts [18, 6]. Our models are trained on a cluster with NVIDIA A100 and V100 GPUs. The inference speed on iPhone 12 (A14 bionic chip) is measured with iOS version 15 and averaged over $1,000$ runs, with all available computing resources (NPU), or CPU only. CoreMLTools is used to deploy the run-time model. In addition, we provide latency analysis on Nvidia A100 GPU with batch size 64 to exploit hardware roofline. The trained PyTorch models are deployed in ONNX format and are compiled with TensorRT. We report GPU runtime that excludes preprocessing. We provide the detailed network architecture and more ablation studies in Appendix 6.

5.1 Image Classification

All EfficientFormer models are trained from scratch on ImageNet-1K dataset [34] to perform the image classification task. We employ standard image size (224×224) for both training and testing. We follow the training recipe from DeiT [3] but mainly report results with 300 training epochs to have the comparison with other ViT-based models. We use AdamW optimizer [75, 76], warm-up training with 5 epochs, and a cosine annealing learning rate schedule. The initial learning rate is set as $10^{-3} \times (batch\ size/1024)$ and the minimum learning rate is 10^{-5}. The teacher model for distillation

Table 1: **Comparison results on ImgeNet-1K.** The latency results are tested on iPhone Neural Engine (NPU), iPhone CPU and Nvidia A100 GPU correspondingly. Note that for mobile speed, we report latency per frame, while on A100 GPU, we report latency per batch size 64 to maximum resource utilization. Hybrid refers to a mixture of MobileNet blocks and ViT blocks. (-) refers to unrevealed or unsupported models. †Latency measured with GeLU activation for fair comparison, the original LeViT-256 model with HardSwish activations runs at 44.5 ms. Different training seeds lead to less than $\pm 0.2\%$ fluctuation in accuracy for EfficientFormer, and the error for latency benchmark is less than ± 0.1 ms.

Model	Type	Params(M)	GMACs	Train. Epoch	Top-1(%)	Latency (ms)		
						NPU	CPU	A100
MobileNetV2×1.0	CONV	3.5	0.3	300	71.8	1.3	8.0	5.0
MobileNetV2×1.4	CONV	6.1	0.6	300	74.7	1.6	10.7	7.3
ResNet50	CONV	25.5	4.1	300	78.5	3.0	29.4	9.0
EfficientNet-B0	CONV	5.3	0.4	350	77.1	2.7	14.5	10.0
EfficientNet-B3	CONV	12.0	1.8	350	81.6	6.6	52.6	35.0
EfficientNet-B5	CONV	30.0	9.9	350	83.6	23.0	258.8	141.0
DeiT-T	Attention	5.9	1.2	300/1000	74.5/76.6	9.2	16.7	7.1
DeiT-S	Attention	22.5	4.5	300/1000	81.2/82.6	11.8	41.0	15.5
PVT-Small	Attention	24.5	3.8	300	79.8	24.4	89.5	23.8
T2T-ViT-14	Attention	21.5	4.8	310	81.5	-	-	21.0
Swin-Tiny	Attention	29	4.5	300	81.3	-	-	22.0
CSwin-T	Attention	23	4.3	300	82.7	-	-	28.7
PoolFormer-s12	Pool	12	2.0	300	77.2	6.1	59.0	14.5
PoolFormer-s24	Pool	21	3.6	300	80.3	6.2	126.7	28.2
PoolFormer-s36	Pool	31	5.2	300	81.4	6.7	192.6	41.2
ResMLP-S24	SMLP	30	6.0	300	79.4	7.6	40.2	17.4
Convmixer-768	Hybrid	21.1	20.7	300	80.2	11.6	29.3	-
LeViT-256	Hybrid	18.9	1.1	1000	81.6	11.9 †	13.5	4.5
NASViT-A5	Hybrid	-	0.76	360	81.8	-	-	-
MobileViT-XS	Hybrid	2.3	0.7	300	74.8	7.2	26.5	11.7
MobileFormer-508M	Hybrid	14.0	0.51	450	79.3	13.2	22.2	14.6
EfficientFormer-L1	MetaBlock	12.3	1.3	300/1000	**79.2/80.2**	**1.6**	**11.5**	**6.2**
EfficientFormer-L3	MetaBlock	31.3	3.9	300	**82.4**	**3.0**	**28.2**	**13.9**
EfficientFormer-L7	MetaBlock	82.1	10.2	300	**83.3**	**7.0**	**67.7**	**30.7**

is RegNetY-16GF [77] pretrained on ImageNet with 82.9% top-1 accuracy. Results are demonstrated in Tab. 1 and Fig. 1

Comparison to CNNs. Compared with the widely used CNN-based models, EfficientFormer achieves a better trade-off between accuracy and latency. On iPhone Neural Engine, EfficientFormer-L1 runs at MobileNetV2×1.4 speed while achieving 4.5% higher top-1 accuracy. In addition, EfficientFormer-L3 runs at a similar speed to EfficientNet-B0 while achieving relative 5.3% higher top-1 accuracy. For the models with high performance ($> 83\%$ top-1), EfficientFormer-L7 runs more than 3× faster than EfficientNet-B5, demonstrating the advantageous performance of our models. Moreover on desktop GPU (A100), EfficientFormer-L1 runs 38% faster than EfficientNet-B0 while achieving 2.1% higher top-1 accuracy. EfficientFormer-L7 runs 4.6× faster than EfficientNet-B5. These results allow us to answer the central question raised earlier; *ViTs do not need to sacrifice latency to achieve good performance, and an accurate ViT can still have ultra-fast inference speed as lightweight CNNs do.*

Comparison to ViTs. Conventional ViTs are still under-performing CNNs in terms of latency. For instance, DeiT-Tiny achieves similar accuracy to EfficientNet-B0 while it runs $3.4\times$ slower. However, EfficientFormer performs like other transformer models while running times faster. EfficientFormer-L3 achieves higher accuracy than DeiT-Small (82.4% *vs.* 81.2%) while being $4\times$ faster. It is notable that though the recent transformer variant, PoolFormer [6], naturally has a consistent 4D architecture and runs faster compared to typical ViTs, the absence of global MHSA greatly limits the performance upper-bound. EfficientFormer-L3 achieves 1% higher top-1 accuracy than PoolFormer-S36, while being 3× faster on Nvidia A100 GPU, 2.2× faster on iPhone NPU and 6.8× faster on iPhone CPU.

Comparison to Hybrid Designs. Existing hybrid designs, *e.g.*, LeViT-256 and MobileViT, still struggle with the latency bottleneck of ViTs and can hardly outperform lightweight CNNs. For example, LeViT-256 runs slower than DeiT-Small while having 1% lower top-1 accuracy. For MobileViT, which is a hybrid model with both MHSA and MobileNet blocks, we observe that it

Table 2: **Comparison results using EfficientFormer as backbone.** Results on object detection & instance segmentation are obtained from COCO 2017. Results on semantic segmentation are obtained from ADE20K.

Backbone	Detection & Instance Segmentation						Semantic
	$\mathbf{AP}^{box}$	$\mathbf{AP}^{box}_{50}$	$\mathbf{AP}^{box}_{75}$	$\mathbf{AP}^{mask}$	$\mathbf{AP}^{mask}_{50}$	$\mathbf{AP}^{mask}_{75}$	mIoU(%)
ResNet18	34.0	54.0	36.7	31.2	51.0	32.7	32.9
PoolFormer-S12	37.3	59.0	40.1	34.6	55.8	36.9	37.2
EfficientFormer-L1	**37.9**	**60.3**	**41.0**	**35.4**	**57.3**	**37.3**	**38.9**
ResNet50	38.0	58.6	41.4	34.4	55.1	36.7	36.7
PoolFormer-S24	40.1	62.2	43.4	37.0	59.1	39.6	40.3
EfficientFormer-L3	**41.4**	**63.9**	**44.7**	**38.1**	**61.0**	**40.4**	**43.5**
ResNet101	40.4	61.1	44.2	36.4	57.7	38.8	38.8
PoolFormer-S36	41.0	63.1	44.8	37.7	60.1	40.0	42.0
EfficientFormer-L7	**42.6**	**65.1**	**46.1**	**39.0**	**62.2**	**41.7**	**45.1**

is significantly slower than CNN counterparts, *e.g.*, MobileNetV2 and EfficientNet-B0, while the accuracy is not satisfactory either (2.3% lower than EfficientNet-B0). Thus, simply trading-off MHSA with MobileNet blocks can hardly push forward the Pareto curve, as in Fig. 1. In contrast, EfficientFormer, as pure transformer-based model, can maintain high performance while achieving ultra-fast inference speed. EfficientFormer-L1 has 4.4% higher top-1 accuracy than MobileViT-XS and runs much faster across different hardware and compilers (1.9× faster on Nvidia A100 GPU Computing, 2.3× faster on iPhone CPU, and 4.5× faster on iPhone NPU). At a similar inference time, EfficientFormer-L7 outperforms MobileViT-XS by 8.5% top-1 accuracy on ImageNet, demonstrating the superiority of our design.

5.2 EfficientFormer as Backbone

Object Detection and Instance Segmentation. We follow the implementation of Mask-RCNN [78] to integrate EfficientFormer as the backbone and verify performance. We experiment over COCO-2017 [79] which contains training and validations sets of 118K and 5K images, respectively. The EfficientFormer backbone is initialized with ImageNet-1K pretrained weights. Similar to prior work [6], we use AdamW optimizer [75, 76] with initial learning rate of 2×10^{-4}, and train the model for 12 epochs. We set the input size as 1333×800.

The results for detection and instance segmentation are shown in Tab. 2. EfficientFormers consistently outperform CNN (ResNet) and transformer (PoolFormer) backbones. With similar computation cost, EfficientFormer-L3 outperforms ResNet50 backbone by 3.4 box **AP** and 3.7 mask **AP**, and outperforms PoolFormer-S24 backbone with 1.3 box **AP** and 1.1 mask **AP**, proving that EfficientFormer generalizes well as a strong backbone in vision tasks.

Semantic Segmentation. We further validate the performance of EfficientFormer on the semantic segmentation task. We use the challenging scene parsing dataset, ADE20K [80, 81], which contains 20K training images and 2K validation ones covering 150 class categories. Similar to existing work [6], we build EfficientFormer as backbone along with Semantic FPN [82] as segmentation decoder for fair comparison. The backbone is initialized with pretrained weights on ImageNet-1K and the model is trained for 40K iterations with a total batch size of 32 over 8 GPUs. We follow the common practice in segmentation [6, 13], use AdamW optimizer [75, 76], and apply a poly learning rate schedule with power 0.9, starting from a initial learning rate 2×10^{-4}. We resize and crop input images to 512×512 for training and shorter side as 512 for testing (on validation set).

As shown in Tab. 2, EfficientFormer consistently outperforms CNN- and transformer-based backbones by a large margin under a similar computation budget. For example, EfficientFormer-L3 outperforms PoolFormer-S24 by 3.2 mIoU. We show that with global attention, EfficientFormer learns better long-term dependencies, which is beneficial in high-resolution dense prediction tasks.

5.3 Discussion

Relations to MetaFormer. The design of EfficientFormer is partly inspired by the MetaFormer concept [6]. Compared to PoolFormer, EfficientFormer addresses the dimension mismatch problem,

which is a root cause of inefficient edge inference, thus being capable of utilizing global MHSA without sacrificing speed. Consequently, EfficientFormer exhibits advantageous accuracy performance over PoolFormer. In spite of its fully 4D design, PoolFormer employs inefficient patch embedding and group normalization (Fig. 2), leading to increased latency. Instead, our redesigned 4D partition of EfficientFormer (Fig. 3) is more hardware friendly and exhibits better performance across several tasks.

Limitations. (i) Though most designs in EfficientFormer are general-purposed, *e.g.*, dimension-consistent design and 4D block with CONV-BN fusion, the actual speed of EfficientFormer may vary on other platforms. For instance, if GeLU is not well supported while HardSwish is efficiently implemented on specific hardware and compiler, the operator may need to be modified accordingly. (ii) The proposed latency-driven slimming is simple and fast. However, better results may be achieved if search cost is not a concern and an enumeration-based brute search is performed.

6 Conclusion

In this work, we show that Vision Transformer can operate at MobileNet speed on mobile devices. Starting from a comprehensive latency analysis, we identify inefficient operators in a series of ViT-based architectures, whereby we draw important observations that guide our new design paradigm. The proposed EfficientFormer complies with a dimension consistent design that smoothly leverages hardware-friendly 4D MetaBlocks and powerful 3D MHSA blocks. We further propose a fast latency-driven slimming method to derive optimized configurations based on our design space. Extensive experiments on image classification, object detection, and segmentation tasks show that EfficientFormer models outperform existing transformer models while being faster than most competitive CNNs. The latency-driven analysis of ViT architecture and the experimental results validate our claim: powerful vision transformers can achieve ultra-fast inference speed on the edge. Future research will further explore the potential of EfficientFormer on several resource-constrained devices.

Acknowledgment

This work is supported in part by National Science Foundation CCF-1937500.

References

[1] Ashish Vaswani, Noam Shazeer, Niki Parmar, Jakob Uszkoreit, Llion Jones, Aidan N Gomez, Łukasz Kaiser, and Illia Polosukhin. Attention is all you need. *Advances in neural information processing systems*, 30, 2017.

[2] Alexey Dosovitskiy, Lucas Beyer, Alexander Kolesnikov, Dirk Weissenborn, Xiaohua Zhai, Thomas Unterthiner, Mostafa Dehghani, Matthias Minderer, Georg Heigold, Sylvain Gelly, Jakob Uszkoreit, and Neil Houlsby. An image is worth 16x16 words: Transformers for image recognition at scale. *ICLR*, 2021.

[3] Hugo Touvron, Matthieu Cord, Matthijs Douze, Francisco Massa, Alexandre Sablayrolles, and Hervé Jégou. Training data-efficient image transformers & distillation through attention. In *International Conference on Machine Learning*, pages 10347–10357. PMLR, 2021.

[4] Hugo Touvron, Matthieu Cord, and Hervé Jégou. Deit iii: Revenge of the vit. *arXiv preprint arXiv:2204.07118*, 2022.

[5] Hugo Touvron, Matthieu Cord, Alaaeldin El-Nouby, Jakob Verbeek, and Hervé Jégou. Three things everyone should know about vision transformers. *arXiv preprint arXiv:2203.09795*, 2022.

[6] Weihao Yu, Mi Luo, Pan Zhou, Chenyang Si, Yichen Zhou, Xinchao Wang, Jiashi Feng, and Shuicheng Yan. Metaformer is actually what you need for vision. *arXiv preprint arXiv:2111.11418*, 2021.

[7] Lingchen Meng, Hengduo Li, Bor-Chun Chen, Shiyi Lan, Zuxuan Wu, Yu-Gang Jiang, and Ser-Nam Lim. Adavit: Adaptive vision transformers for efficient image recognition. *arXiv preprint arXiv:2111.15668*, 2021.

[8] Ze Liu, Yutong Lin, Yue Cao, Han Hu, Yixuan Wei, Zheng Zhang, Stephen Lin, and Baining Guo. Swin transformer: Hierarchical vision transformer using shifted windows. In *Proceedings of the IEEE/CVF International Conference on Computer Vision*, pages 10012–10022, 2021.

[9] Sebastian Jaszczur, Aakanksha Chowdhery, Afroz Mohiuddin, Lukasz Kaiser, Wojciech Gajewski, Henryk Michalewski, and Jonni Kanerva. Sparse is enough in scaling transformers. *Advances in Neural Information Processing Systems*, 34:9895–9907, 2021.

[10] Ze Liu, Han Hu, Yutong Lin, Zhuliang Yao, Zhenda Xie, Yixuan Wei, Jia Ning, Yue Cao, Zheng Zhang, Li Dong, et al. Swin transformer v2: Scaling up capacity and resolution. *arXiv preprint arXiv:2111.09883*, 2021.

[11] Ze Liu, Jia Ning, Yue Cao, Yixuan Wei, Zheng Zhang, Stephen Lin, and Han Hu. Video swin transformer. *arXiv preprint arXiv:2106.13230*, 2021.

[12] Mathilde Caron, Hugo Touvron, Ishan Misra, Hervé Jégou, Julien Mairal, Piotr Bojanowski, and Armand Joulin. Emerging properties in self-supervised vision transformers. In *Proceedings of the IEEE/CVF International Conference on Computer Vision*, pages 9650–9660, 2021.

[13] Enze Xie, Wenhai Wang, Zhiding Yu, Anima Anandkumar, Jose M Alvarez, and Ping Luo. Segformer: Simple and efficient design for semantic segmentation with transformers. *arXiv preprint arXiv:2105.15203*, 2021.

[14] Bowen Cheng, Ishan Misra, Alexander G Schwing, Alexander Kirillov, and Rohit Girdhar. Masked-attention mask transformer for universal image segmentation. *arXiv preprint arXiv:2112.01527*, 2021.

[15] Nicolas Carion, Francisco Massa, Gabriel Synnaeve, Nicolas Usunier, Alexander Kirillov, and Sergey Zagoruyko. End-to-end object detection with transformers. In *European conference on computer vision*, pages 213–229. Springer, 2020.

[16] Yanghao Li, Chao-Yuan Wu, Haoqi Fan, Karttikeya Mangalam, Bo Xiong, Jitendra Malik, and Christoph Feichtenhofer. Improved multiscale vision transformers for classification and detection. *arXiv preprint arXiv:2112.01526*, 2021.

[17] Xudong Wang, Li Lyna Zhang, Yang Wang, and Mao Yang. Towards efficient vision transformer inference: a first study of transformers on mobile devices. In *Proceedings of the 23rd Annual International Workshop on Mobile Computing Systems and Applications*, pages 1–7, 2022.

[18] Sachin Mehta and Mohammad Rastegari. Mobilevit: Light-weight, general-purpose, and mobile-friendly vision transformer. *arXiv preprint arXiv:2110.02178*, 2021.

[19] Xingyu Liu, Jeff Pool, Song Han, and William J Dally. Efficient sparse-winograd convolutional neural networks. *arXiv preprint arXiv:1802.06367*, 2018.

[20] Andrew G Howard, Menglong Zhu, Bo Chen, Dmitry Kalenichenko, Weijun Wang, Tobias Weyand, Marco Andreetto, and Hartwig Adam. Mobilenets: Efficient convolutional neural networks for mobile vision applications. *arXiv preprint arXiv:1704.04861*, 2017.

[21] Mark Sandler, Andrew Howard, Menglong Zhu, Andrey Zhmoginov, and Liang-Chieh Chen. Mobilenetv2: Inverted residuals and linear bottlenecks. In *Proceedings of the IEEE conference on computer vision and pattern recognition*, pages 4510–4520, 2018.

[22] Andrew Howard, Mark Sandler, Grace Chu, Liang-Chieh Chen, Bo Chen, Mingxing Tan, Weijun Wang, Yukun Zhu, Ruoming Pang, Vijay Vasudevan, et al. Searching for mobilenetv3. In *Proceedings of the IEEE/CVF International Conference on Computer Vision*, pages 1314–1324, 2019.

[23] Benjamin Graham, Alaaeldin El-Nouby, Hugo Touvron, Pierre Stock, Armand Joulin, Herve Jegou, and Matthijs Douze. Levit: A vision transformer in convnet's clothing for faster inference. In *Proceedings of the IEEE/CVF International Conference on Computer Vision (ICCV)*, pages 12259–12269, October 2021.

[24] Yinpeng Chen, Xiyang Dai, Dongdong Chen, Mengchen Liu, Xiaoyi Dong, Lu Yuan, and Zicheng Liu. Mobile-former: Bridging mobilenet and transformer. *arXiv preprint arXiv:2108.05895*, 2021.

[25] Chuhan Wu, Fangzhao Wu, Tao Qi, Binxing Jiao, Daxin Jiang, Yongfeng Huang, and Xing Xie. Smart bird: Learnable sparse attention for efficient and effective transformer. *arXiv preprint arXiv:2108.09193*, 2021.

[26] Byungseok Roh, JaeWoong Shin, Wuhyun Shin, and Saehoon Kim. Sparse detr: Efficient end-to-end object detection with learnable sparsity. *arXiv preprint arXiv:2111.14330*, 2021.

[27] Xizhou Zhu, Weijie Su, Lewei Lu, Bin Li, Xiaogang Wang, and Jifeng Dai. Deformable detr: Deformable transformers for end-to-end object detection. *arXiv preprint arXiv:2010.04159*, 2020.

[28] Chengyue Gong, Dilin Wang, Meng Li, Xinlei Chen, Zhicheng Yan, Yuandong Tian, qiang liu, and Vikas Chandra. NASVit: Neural architecture search for efficient vision transformers with gradient conflict aware supernet training. In *International Conference on Learning Representations*, 2022.

[29] Arnav Chavan, Zhiqiang Shen, Zhuang Liu, Zechun Liu, Kwang-Ting Cheng, and Eric Xing. Vision transformer slimming: Multi-dimension searching in continuous optimization space. 2022.

[30] CoreMLTools. Use coremltools to convert models from third-party libraries to core ml., 2021.

[31] Ningning Ma, Xiangyu Zhang, Hai-Tao Zheng, and Jian Sun. Shufflenet v2: Practical guidelines for efficient cnn architecture design. In *Proceedings of the European conference on computer vision (ECCV)*, pages 116–131, 2018.

[32] Mingxing Tan, Bo Chen, Ruoming Pang, Vijay Vasudevan, Mark Sandler, Andrew Howard, and Quoc V Le. Mnasnet: Platform-aware neural architecture search for mobile. In *Proceedings of the IEEE/CVF Conference on Computer Vision and Pattern Recognition*, pages 2820–2828, 2019.

[33] Hanrui Wang, Zhanghao Wu, Zhijian Liu, Han Cai, Ligeng Zhu, Chuang Gan, and Song Han. Hat: Hardware-aware transformers for efficient natural language processing. *arXiv preprint arXiv:2005.14187*, 2020.

[34] Jia Deng, Wei Dong, Richard Socher, Li-Jia Li, Kai Li, and Li Fei-Fei. Imagenet: A large-scale hierarchical image database. In *2009 IEEE conference on computer vision and pattern recognition*, pages 248–255. Ieee, 2009.

[35] Li Yuan, Yunpeng Chen, Tao Wang, Weihao Yu, Yujun Shi, Zi-Hang Jiang, Francis EH Tay, Jiashi Feng, and Shuicheng Yan. Tokens-to-token vit: Training vision transformers from scratch on imagenet. In *Proceedings of the IEEE/CVF International Conference on Computer Vision*, pages 558–567, 2021.

[36] Wenhai Wang, Enze Xie, Xiang Li, Deng-Ping Fan, Kaitao Song, Ding Liang, Tong Lu, Ping Luo, and Ling Shao. Pyramid vision transformer: A versatile backbone for dense prediction without convolutions. In *Proceedings of the IEEE/CVF International Conference on Computer Vision*, pages 568–578, 2021.

[37] Hugo Touvron, Matthieu Cord, Alexandre Sablayrolles, Gabriel Synnaeve, and Hervé Jégou. Going deeper with image transformers. In *Proceedings of the IEEE/CVF International Conference on Computer Vision*, pages 32–42, 2021.

[38] Jianyuan Guo, Kai Han, Han Wu, Chang Xu, Yehui Tang, Chunjing Xu, and Yunhe Wang. Cmt: Convolutional neural networks meet vision transformers. *arXiv preprint arXiv:2107.06263*, 2021.

[39] Zihang Dai, Hanxiao Liu, Quoc V Le, and Mingxing Tan. Coatnet: Marrying convolution and attention for all data sizes. *Advances in Neural Information Processing Systems*, 34:3965–3977, 2021.

[40] Qi Han, Zejia Fan, Qi Dai, Lei Sun, Ming-Ming Cheng, Jiaying Liu, and Jingdong Wang. On the connection between local attention and dynamic depth-wise convolution. In *International Conference on Learning Representations*, 2021.

[41] Zizhao Zhang, Han Zhang, Long Zhao, Ting Chen, Sercan Arik, and Tomas Pfister. Nested hierarchical transformer: Towards accurate, data-efficient and interpretable visual understanding. 2022.

[42] Wenqiang Zhang, Zilong Huang, Guozhong Luo, Tao Chen, Xinggang Wang, Wenyu Liu, Gang Yu, and Chunhua Shen. Topformer: Token pyramid transformer for mobile semantic segmentation, 2022.

[43] Seung Hoon Lee, Seunghyun Lee, and Byung Cheol Song. Vision transformer for small-size datasets. *arXiv preprint arXiv:2112.13492*, 2021.

[44] Kwonjoon Lee, Huiwen Chang, Lu Jiang, Han Zhang, Zhuowen Tu, and Ce Liu. Vitgan: Training gans with vision transformers. *arXiv preprint arXiv:2107.04589*, 2021.

[45] Patrick Esser, Robin Rombach, and Bjorn Ommer. Taming transformers for high-resolution image synthesis. In *Proceedings of the IEEE/CVF Conference on Computer Vision and Pattern Recognition*, pages 12873–12883, 2021.

[46] Yanhong Zeng, Huan Yang, Hongyang Chao, Jianbo Wang, and Jianlong Fu. Improving visual quality of image synthesis by a token-based generator with transformers. *Advances in Neural Information Processing Systems*, 34, 2021.

[47] Hugo Touvron, Piotr Bojanowski, Mathilde Caron, Matthieu Cord, Alaaeldin El-Nouby, Edouard Grave, Gautier Izacard, Armand Joulin, Gabriel Synnaeve, Jakob Verbeek, et al. Resmlp: Feedforward networks for image classification with data-efficient training. *arXiv preprint arXiv:2105.03404*, 2021.

[48] Ilya Tolstikhin, Neil Houlsby, Alexander Kolesnikov, Lucas Beyer, Xiaohua Zhai, Thomas Unterthiner, Jessica Yung, Andreas Steiner, Daniel Keysers, Jakob Uszkoreit, Mario Lucic, and Alexey Dosovitskiy. Mlp-mixer: An all-mlp architecture for vision. *arXiv preprint arXiv:2105.01601*, 2021.

[49] Mingxing Tan and Quoc Le. Efficientnet: Rethinking model scaling for convolutional neural networks. In *International conference on machine learning*, pages 6105–6114. PMLR, 2019.

[50] Ilya O Tolstikhin, Neil Houlsby, Alexander Kolesnikov, Lucas Beyer, Xiaohua Zhai, Thomas Unterthiner, Jessica Yung, Andreas Steiner, Daniel Keysers, Jakob Uszkoreit, et al. Mlp-mixer: An all-mlp architecture for vision. *Advances in Neural Information Processing Systems*, 34, 2021.

[51] Shoufa Chen, Enze Xie, Chongjian Ge, Ding Liang, and Ping Luo. Cyclemlp: A mlp-like architecture for dense prediction. *arXiv preprint arXiv:2107.10224*, 2021.

[52] Daquan Zhou, Bingyi Kang, Xiaojie Jin, Linjie Yang, Xiaochen Lian, Zihang Jiang, Qibin Hou, and Jiashi Feng. Deepvit: Towards deeper vision transformer. *arXiv preprint arXiv:2103.11886*, 2021.

[53] Nikita Kitaev, Lukasz Kaiser, and Anselm Levskaya. Reformer: The efficient transformer. In *ICLR*. OpenReview.net, 2020.

[54] Chun-Fu Richard Chen, Quanfu Fan, and Rameswar Panda. Crossvit: Cross-attention multi-scale vision transformer for image classification. In *Proceedings of the IEEE/CVF International Conference on Computer Vision*, pages 357–366, 2021.

[55] Ali Hassani, Steven Walton, Nikhil Shah, Abulikemu Abuduweili, Jiachen Li, and Humphrey Shi. Escaping the big data paradigm with compact transformers. *arXiv preprint arXiv:2104.05704*, 2021.

[56] Mohsen Fayyaz, Soroush Abbasi Kouhpayegani, Farnoush Rezaei Jafari, Eric Sommerlade, Hamid Reza Vaezi Joze, Hamed Pirsiavash, and Juergen Gall. Ats: Adaptive token sampling for efficient vision transformers. *arXiv preprint arXiv:2111.15667*, 2021.

[57] Wei Li, Xing Wang, Xin Xia, Jie Wu, Xuefeng Xiao, Min Zheng, and Shiping Wen. Sepvit: Separable vision transformer. *CoRR*, abs/2203.15380, 2022.

[58] Cédric Renggli, André Susano Pinto, Neil Houlsby, Basil Mustafa, Joan Puigcerver, and Carlos Riquelme. Learning to merge tokens in vision transformers. *CoRR*, abs/2202.12015, 2022.

[59] Wenxiao Wang, Lu Yao, Long Chen, Binbin Lin, Deng Cai, Xiaofei He, and Wei Liu. Crossformer: A versatile vision transformer hinging on cross-scale attention. *arXiv preprint arXiv:2108.00154*, 2021.

[60] Byeongho Heo, Sangdoo Yun, Dongyoon Han, Sanghyuk Chun, Junsuk Choe, and Seong Joon Oh. Rethinking spatial dimensions of vision transformers. In *Proceedings of the IEEE/CVF International Conference on Computer Vision*, pages 11936–11945, 2021.

[61] Chun-Fu Chen, Rameswar Panda, and Quanfu Fan. Regionvit: Regional-to-local attention for vision transformers. *arXiv preprint arXiv:2106.02689*, 2021.

[62] Yawei Li, Kai Zhang, Jiezhang Cao, Radu Timofte, and Luc Van Gool. Localvit: Bringing locality to vision transformers. *arXiv preprint arXiv:2104.05707*, 2021.

[63] Xiangxiang Chu, Zhi Tian, Yuqing Wang, Bo Zhang, Haibing Ren, Xiaolin Wei, Huaxia Xia, and Chunhua Shen. Twins: Revisiting spatial attention design in vision transformers. *arXiv e-prints*, pages arXiv–2104, 2021.

[64] Yongming Rao, Wenliang Zhao, Benlin Liu, Jiwen Lu, Jie Zhou, and Cho-Jui Hsieh. Dynamicvit: Efficient vision transformers with dynamic token sparsification. In *Advances in Neural Information Processing Systems (NeurIPS)*, 2021.

[65] Zhengzhong Tu, Hossein Talebi, Han Zhang, Feng Yang, Peyman Milanfar, Alan Bovik, and Yinxiao Li. Maxvit: Multi-axis vision transformer. *CoRR*, abs/2204.01697, 2022.

[66] Minghao Chen, Houwen Peng, Jianlong Fu, and Haibin Ling. Autoformer: Searching transformers for visual recognition. In *Proceedings of the IEEE/CVF International Conference on Computer Vision*, pages 12270–12280, 2021.

[67] Qinqin Zhou, Kekai Sheng, Xiawu Zheng, Ke Li, Xing Sun, Yonghong Tian, Jie Chen, and Rongrong Ji. Training-free transformer architecture search. *arXiv preprint arXiv:2203.12217*, 2022.

[68] Haiping Wu, Bin Xiao, Noel Codella, Mengchen Liu, Xiyang Dai, Lu Yuan, and Lei Zhang. Cvt: Introducing convolutions to vision transformers. In *Proceedings of the IEEE/CVF International Conference on Computer Vision*, pages 22–31, 2021.

[69] Kun Yuan, Shaopeng Guo, Ziwei Liu, Aojun Zhou, Fengwei Yu, and Wei Wu. Incorporating convolution designs into visual transformers. In *Proceedings of the IEEE/CVF International Conference on Computer Vision*, pages 579–588, 2021.

[70] Asher Trockman and J Zico Kolter. Patches are all you need? *arXiv preprint arXiv:2201.09792*, 2022.

[71] Tien-Ju Yang, Andrew Howard, Bo Chen, Xiao Zhang, Alec Go, Mark Sandler, Vivienne Sze, and Hartwig Adam. Netadapt: Platform-aware neural network adaptation for mobile applications. In *Proceedings of the European Conference on Computer Vision (ECCV)*, pages 285–300, 2018.

[72] Hanxiao Liu, Karen Simonyan, and Yiming Yang. Darts: Differentiable architecture search. *arXiv preprint arXiv:1806.09055*, 2018.

[73] Adam Paszke, Sam Gross, Francisco Massa, Adam Lerer, James Bradbury, Gregory Chanan, Trevor Killeen, Zeming Lin, Natalia Gimelshein, Luca Antiga, et al. Pytorch: An imperative style, high-performance deep learning library. *Advances in neural information processing systems*, 32, 2019.

[74] Ross Wightman. Pytorch image models. `https://github.com/rwightman/pytorch-image-models`, 2019.

[75] Diederik P Kingma and Jimmy Ba. Adam: A method for stochastic optimization. *arXiv preprint arXiv:1412.6980*, 2014.

[76] Ilya Loshchilov and Frank Hutter. Decoupled weight decay regularization. *arXiv preprint arXiv:1711.05101*, 2017.

[77] Ilija Radosavovic, Raj Prateek Kosaraju, Ross Girshick, Kaiming He, and Piotr Dollár. Designing network design spaces. In *Proceedings of the IEEE/CVF Conference on Computer Vision and Pattern Recognition*, pages 10428–10436, 2020.

[78] Kaiming He, Georgia Gkioxari, Piotr Dollár, and Ross Girshick. Mask r-cnn. In *Proceedings of the IEEE international conference on computer vision*, pages 2961–2969, 2017.

[79] Tsung-Yi Lin, Michael Maire, Serge Belongie, James Hays, Pietro Perona, Deva Ramanan, Piotr Dollár, and C Lawrence Zitnick. Microsoft coco: Common objects in context. In *European conference on computer vision*, pages 740–755. Springer, 2014.

[80] Bolei Zhou, Hang Zhao, Xavier Puig, Sanja Fidler, Adela Barriuso, and Antonio Torralba. Scene parsing through ade20k dataset. In *Proceedings of the IEEE Conference on Computer Vision and Pattern Recognition*, 2017.

[81] Bolei Zhou, Hang Zhao, Xavier Puig, Tete Xiao, Sanja Fidler, Adela Barriuso, and Antonio Torralba. Semantic understanding of scenes through the ade20k dataset. *International Journal of Computer Vision*, 127(3):302–321, 2019.

[82] Alexander Kirillov, Ross Girshick, Kaiming He, and Piotr Dollár. Panoptic feature pyramid networks. In *Proceedings of the IEEE/CVF Conference on Computer Vision and Pattern Recognition*, pages 6399–6408, 2019.

Checklist

1. For all authors...
   (a) Do the main claims made in the abstract and introduction accurately reflect the paper's contributions and scope? [Yes]
   (b) Did you describe the limitations of your work? [Yes]
   (c) Did you discuss any potential negative societal impacts of your work? [Yes]
   (d) Have you read the ethics review guidelines and ensured that your paper conforms to them? [Yes]
2. If you are including theoretical results...
   (a) Did you state the full set of assumptions of all theoretical results? [N/A]
   (b) Did you include complete proofs of all theoretical results? [N/A]
3. If you ran experiments...
   (a) Did you include the code, data, and instructions needed to reproduce the main experimental results (either in the supplemental material or as a URL)? [Yes]
   (b) Did you specify all the training details (e.g., data splits, hyperparameters, how they were chosen)? [Yes]
   (c) Did you report error bars (e.g., with respect to the random seed after running experiments multiple times)? [Yes]
   (d) Did you include the total amount of compute and the type of resources used (e.g., type of GPUs, internal cluster, or cloud provider)? [Yes]
4. If you are using existing assets (e.g., code, data, models) or curating/releasing new assets...
   (a) If your work uses existing assets, did you cite the creators? [Yes]
   (b) Did you mention the license of the assets? [Yes]
   (c) Did you include any new assets either in the supplemental material or as a URL? [N/A]
   (d) Did you discuss whether and how consent was obtained from people whose data you're using/curating? [N/A]
   (e) Did you discuss whether the data you are using/curating contains personally identifiable information or offensive content? [N/A]
5. If you used crowdsourcing or conducted research with human subjects...
   (a) Did you include the full text of instructions given to participants and screenshots, if applicable? [N/A]
   (b) Did you describe any potential participant risks, with links to Institutional Review Board (IRB) approvals, if applicable? [N/A]
   (c) Did you include the estimated hourly wage paid to participants and the total amount spent on participant compensation? [N/A]

Appendix

A Latency-Driven Slimming Algorithm

We provide the details of the proposed latency-driven fast slimming in Alg. 1. Formulations of the algorithm can be found in Sec. 4.2. The proposed latency-driven slimming is speed-oriented, which does not require retraining for each sub-network. The importance score for each design choice is estimated based on the trainable architecture parameter α.

Algorithm 1 Fast Latency-Driven Slimming based on Importance Estimations

Require: Latency lookup table $T = \{\texttt{MB}^{4D}\{dim = 16\times\}, \texttt{MB}^{3D}\{dim = 16\times\}\}$
Ensure: Final latency satisfy budget $\sum T \approx \mathcal{T}$
Super-net Pretraining:
for epoch **do**
  for each iter **do**
    for $\texttt{MP}_{i,j}$ **do**
      $\mathcal{X}_{i+1} = \sum_n \frac{e^{(\alpha_i^n + \epsilon_i^n)/\tau}}{\sum_n e^{(\alpha_i^n + \epsilon_i^n)/\tau}} \cdot \texttt{MP}_{i,j}(\mathcal{X}_i)$,
    end for
    $\mathcal{L} \leftarrow criterion(\mathcal{Y}, label)$
    backpropagate ($\mathcal{L}$), update parameters
  end for
end for ▷ get super-net
Latency-driven slimming:
Initialize action space A ∈ {Depth Reduction (DR), Width Reduction (WR), $\texttt{MB}^{3D}$ Reduction (MR)}
Compute importance of $\texttt{MP}_{i,j}$ by $\mathbb{I}_{i,j} = \frac{\alpha_i^{4D}}{\alpha_i^I}, or \frac{\alpha_i^{3D} + \alpha_i^{4D}}{\alpha_i^I}$
while $\sum T > \mathcal{T}$ **do**

$$\text{DR} \leftarrow \underset{\mathbb{I}_{i,j}}{\operatorname{argmin}}(\texttt{MP}_{i,j}), \quad \text{WR} \leftarrow \underset{\sum_j \mathbb{I}_{i,j}}{\operatorname{argmin}}(\texttt{MP}_{i,j}), \quad \text{MR} \leftarrow \text{First} - \texttt{MB}^{3D},$$

$$\text{Execute Action} = \underset{\frac{\text{accuracy drop}}{T_{i,j}}}{\operatorname{argmin}}(A)$$

end while ▷ get sub-net with target latency
Train the searched architecture from scratch:
Similar to super-net training. ▷ get final model

B Ablation Analysis

Our major conclusions and speed analysis can be found in Sec. 3 and Fig. 2. Here we include more ablation studies for different design choices, provided in Tab. 3, taking the EfficientFormer-L3 as an example. The latency is measured on iPhone 12 with CoreML, and the top-1 accuracy is obtained from the ImageNet-1K dataset.

Patch Embedding. Compared to non-overlap large-kernel patch embedding (V5 in Tab. 3), the proposed convolution stem in EfficientFormer (V1 in Tab. 3) greatly reduces inference latency by 48%, while provides 0.7% higher accuracy. We demonstrate that convolution stem [23] is not only beneficial to model convergence and accuracy but also boosts inference speed on the mobile device by a large margin, thus can serve as a good alternative to non-overlapping patch embedding implementations.

MHSA and Latency-Driven Search. Without the proposed 3D MHSA and latency-driven search, EfficientFormer downgrades to a pure 4D design with pool mixer, which is similar to PoolFormer [6] (the patch embeddings and normalizations are different). By comparing EfficientFormer with V1 in Tab. 3, we can observe that the integration of 3D MHSA and latency-driven search greatly boost

top-1 accuracy by 2.1% with minimal impact on the inference speed (0.5 ms). The results prove that MHSA with the global receptive field is an essential contribution to model performance. As a result, though enjoying faster inference speed, simply removing MHSA [6] greatly limits the performance upper bound. In EfficientFormer, we smoothly integrate MHSA in a dimension consistent manner, obtaining better performance while simultaneously achieving ultra fast inference speed.

Normalization. Apart from the CONV-BN structure in the 4D partition of EfficientFormer, we explore Group Normalization (GN) and channel-wise Layer Normalization (LN) in the 4D partition as employed in the prior work [6]. By comparing V1 and V2 in Tab. 3, we can observe that the GN (V2-GN) can only slightly improve accuracy (0.3% top-1) but incurs latency overhead as it can not be folded at the inference stage. Similarly, applying LN (V2-LN) gets higher latency than BN while the performance improvement is negligible. As a result, we apply the CONV-BN structure in the entire 4D partition in EfficientFormer.

Activation Functions. We explore ReLU and HardSwish (V3 and V4 in Tab. 3) in addition to GeLU employed in this work (V1 in Tab. 3). It is widely agreed that ReLU is the simplest and fastest activation function, while GeLU and HardSwish wield better performance. We observe that ReLU can hardly provide any speedup over GeLU on iPhone 12 with CoreMLTools, while HardSwish is significantly slower than ReLU and GeLU. We draw a conclusion that the activation function can be selected on a case-by-case basis depending on the specific hardware and compiler. In this work, we use GeLU to provide better performance than ReLU while executing faster. For a fair comparison, we modify inefficient operators in other works according to the supports from iPhone 12 and CoreMLTools, *e.g.*, report LeViT latency by changing HardSwish to GeLU.

Dimension Consistent Design. We perform the latency analysis on the Nvidia A100 GPU to show that the proposed dimension-consistent (D-C) design is beneficial besides the iPhone. We deploy the PyTorch models with batch size 64 as ONNX format and use TensorRT to compile and benchmark the latency. We report the latency results averaged over $1,000$ runs in Tab. 4. For the non-D-C design, we revert the proposed Meta3D block into 4D implementation, where linear projections and MLPs are all implemented with CONV1×1-BN instead of 3D-Linear layers, and reshaping operations become necessary in order to perform multi-head self-attention. With this configuration, attention blocks can be arbitrarily placed along with Meta4D blocks without following dimension-consistent design, while frequent reshaping is introduced. We conduct the comparison on the following two models, both with a D-C version and a non-D-C one with the exact same computation complexity:

- EfficientFormer-L7, which has 8 attention blocks.
- DummyNet, a handcrafted dummy model with a total of 16 attention blocks.

As can be seen from Tab. 4, the proposed dimension-consistent design achieves faster inference speed than the non-dimension-consistent design for both EfficientFormer-L7 and the DummyNet.

Latency Driven Slimming. Besides the hardware-efficient architecture design, it is still crucial to find appropriate depth and width configurations for the model to achieve satisfactory performance. To understand the benefits of our latency driven slimming, we randomly sample networks from our search space that have the same computation, *i.e.*, 1.3 GMACs, as our searched model EfficientFormer-L1. The sampled networks are denoted as Random 1 to Random 5, which are either deeper and narrower, or shallower and wider than EfficientFormer-L1. We train the sampled models on ImageNet-1K with the same training recipe as EfficientFormer-L1. The comparison between these models is shown in Tab. 5. As can be seen, our searched EfficientFormer-L1 has better latency or higher top-1 accuracy on ImageNet-1K than the randomly sampled networks, proving the advantages of our proposed latency driven slimming.

C Analysis of Hardware Utilization

EfficientFormer improves the latency vs. accuracy trade-off through better architecture design so that higher hardware utilization is achieved. To understand hardware utilization, we employ throughput in TFLOPS (Tera FLOPs per Second) as the evaluation metric, which is calculated by model computation cost (FLOPs) divided by execution time. Models with higher throughput (TFLOPS) better exploit the computation power of the hardware.

Table 3: Ablation analysis for the design choice on EfficientFormer-L3. V1-5 refers to variants with different operator selections.

Model	CONV stem	Norm.	Activation	MHSA Search	Top-1	Latency (ms)
EfficientFormer	✓	BN	GeLU	✓	82.4	3.0
V1	✓	BN	GeLU		80.3	2.5
V2-GN	✓	GN	GeLU		80.6	3.0
V2-LN	✓	LN	GeLU		80.3	3.7
V3	✓	BN	ReLU		79.3	2.5
V4	✓	BN	HardSwish		80.3	32.4
V5		BN	GeLU		79.6	5.8

Table 4: Analysis of dimension-consistent (D-C) design vs. non-D-C placement of attention blocks. The latency (ms) is measured on the Nvidia A100 GPU with TensorRT.

Model	D-C	TensorRT-A100 (ms)
EfficientFormer-L7	Y	30.67
EfficientFormer-L7	N	34.73
DummyNet	Y	7.07
DummyNet	N	11.93

Table 5: Analysis of latency driven slimming. All random networks are trained with the same training strategy as the EfficientFormer-L1 on ImageNet-1K. The latency is obtained on iPhone 12 NPU with CoreMLTools.

Model	GMACs	Latency (ms)	Top-1 (%)
EfficientFormer-L1	1.3	1.6	79.2
Random 1	1.3	1.6	77.8
Random 2	1.3	1.7	78.3
Random 3	1.3	1.5	74.7
Random 4	1.3	1.6	73.3
Random 5	1.3	1.5	76.7

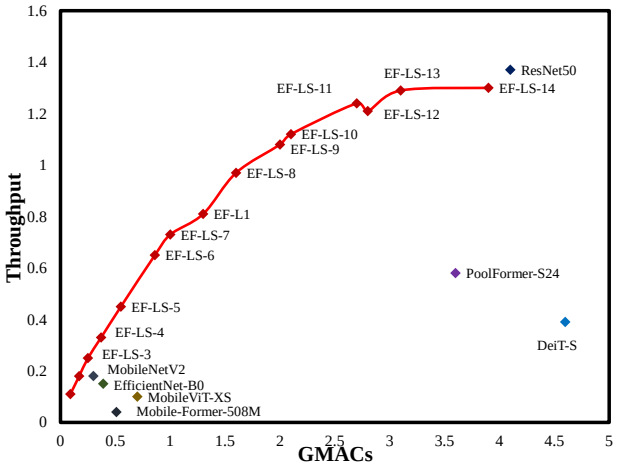

Figure 4: Analysis of hardware utilization on iPhone 12 NPU.

Table 6: Architecture details of EfficientFormer. Exp refers to the expansion ratio of the MLP block. D_{QK} is the dimension of Queries and Keys.

Stage	Resolution	Type	Config	EfficientFormer		
				L1	L3	L7
stem	$\frac{H}{2} \times \frac{W}{2}$	Patch Embed.	Patch Size	$k = 3 \times 3, s = 2$		
			Embed. Dim.	24	32	48
	$\frac{H}{4} \times \frac{W}{4}$	Patch Embed.	Patch Size,	$k = 3 \times 3, s = 2$		
			Embed. Dim.	48	64	96
1	$\frac{H}{4} \times \frac{W}{4}$	$\texttt{MB}^{4D}$	Token Mixer	Pool		
			$\begin{bmatrix} Embed. & Kernel \\ Stride & Exp \end{bmatrix}$	$\begin{bmatrix} 48 & 3 \\ 1 & 4 \end{bmatrix} \times 3$	$\begin{bmatrix} 64 & 3 \\ 1 & 4 \end{bmatrix} \times 4$	$\begin{bmatrix} 96 & 3 \\ 1 & 4 \end{bmatrix} \times 6$
2	$\frac{H}{8} \times \frac{W}{8}$	Patch Embed.	Patch Size	$k = 3 \times 3, s = 2$		
			Embed. Dim.	96	128	192
		$\texttt{MB}^{4D}$	Token Mixer	Pool		
			$\begin{bmatrix} Embed. & Kernel \\ Stride & Exp \end{bmatrix}$	$\begin{bmatrix} 96 & 3 \\ 1 & 4 \end{bmatrix} \times 2$	$\begin{bmatrix} 128 & 3 \\ 1 & 4 \end{bmatrix} \times 4$	$\begin{bmatrix} 192 & 3 \\ 1 & 4 \end{bmatrix} \times 6$
3	$\frac{H}{16} \times \frac{W}{16}$	Patch Embed.	Patch Size	$k = 3 \times 3, s = 2$		
			Embed. Dim.	224	320	384
		$\texttt{MB}^{4D}$	Token Mixer	Pool		
			$\begin{bmatrix} Embed. & Kernel \\ Stride & Exp \end{bmatrix}$	$\begin{bmatrix} 224 & 3 \\ 1 & 4 \end{bmatrix} \times 6$	$\begin{bmatrix} 320 & 3 \\ 1 & 4 \end{bmatrix} \times 12$	$\begin{bmatrix} 384 & 3 \\ 1 & 4 \end{bmatrix} \times 8$
4	$\frac{H}{32} \times \frac{W}{32}$	Patch Embed.	Patch Size	$k = 3 \times 3, s = 2$		
			Embed. Dim.	448	512	768
		$\texttt{MB}^{4D}$	Token Mixer	Pool		
			$\begin{bmatrix} Embed. & Kernel \\ Stride & Exp \end{bmatrix}$	$\begin{bmatrix} 448 & 3 \\ 1 & 4 \end{bmatrix} \times 3$	$\begin{bmatrix} 512 & 3 \\ 1 & 4 \end{bmatrix} \times 3$	$\begin{bmatrix} 768 & 3 \\ 1 & 4 \end{bmatrix} \times 0$
	$\frac{HW}{32^2}$	$\texttt{MB}^{3D}$	Token Mixer	MHSA		
			$\begin{bmatrix} Embed. & D_{QK} \\ Heads & Exp \end{bmatrix}$	$\begin{bmatrix} 448 & 32 \\ 8 & 4 \end{bmatrix} \times 1$	$\begin{bmatrix} 512 & 32 \\ 8 & 4 \end{bmatrix} \times 3$	$\begin{bmatrix} 768 & 32 \\ 8 & 4 \end{bmatrix} \times 8$

To fairly compare with baseline models under different computation complexity, we **L**inearly **S**cale the depth and width of EfficientFormer-L1 to obtain a series of models (EfficientFormer-LS-1 to EfficientFormer-LS-14), with the number of parameters ranging from 1.1M to 31.3M and MACs from 0.09G to 3.9G, and benchmark the latency and utilization on iPhone 12 NPU.

As in Fig. 4, super-tiny models still run at about 1ms, such as EfficientFormer-LS-{1, 2, 3}, where the throughput is low and the hardware is not fully exploited. Data processing and transferring become the bottleneck. As a result, making the model super small with sacrificed accuracy is less valuable. In contrast, our 1.3GMACs model, EfficientFormer-L1 lies at a sweet point, enjoying fast inference speed (1.6ms) while maintaining high accuracy.

Furthermore, we can observe that EfficientFormer variants outperform both CNNs and ViTs in hardware utilization across different computation complexity levels. For instance, at 4-GMACs level, EfficientFormer-LS-14 outperforms DeiT-S by 3.3× higher TFLOPS and outperforms PoolFormer by 2.2×, achieving comparable throughput to ResNet50. In the lightweight domain, EfficientFormer-LS-4 has 2.2× higher TFLOPS than EfficientNet-B0. We demonstrate that with the proposed hardware-friendly design, EfficientFormer naturally has better hardware utilization.

D Architecture of EfficientFormers

The detailed network archiecture for EfficientFormer-L1, EfficientFormer-L3, and EfficientFormer-L7 is provided in Tab. 6. We report the resolution and number of blocks for each stage. In addition, the width of EfficientFormer is specified as the embedding dimension (Embed. Dim.). As for the MHSA block, the dimension of Query and Key is provided, and we employ eight heads for all EfficientFormer variants. MLP expansion ratio is set as default (4), as in most ViT arts [3].